JOURNAL OF SOLID STATE CHEMISTRY 72, 80–91 (1988)

Absorption and Luminescence of Photochromic CdI_2 : CuI*

C. R. RONDA,† E. ZWAAL, H. F. FOLKERSMA, A. LENSELINK, AND C. HAAS

Laboratory of Inorganic Chemistry, Materials Science Centre of the University, Nijenborgh 16, 9747 AG Groningen, The Netherlands

Received February 12, 1987

The irradiation with ultraviolet light of CdI_2 containing 1–5 mole% CuI induces new absorption bands in the visible part of the spectrum. The absorption spectra of uncolored, optically colored, and thermally bleached CdI_2 : CuI are presented and discussed. The optical coloration is due to the photoneutralization of Cu^+ ions in CdI_2, and the thermal bleaching is due to thermal ionization of Cu atoms. During the coloration process small microcrystals of metallic Cu are formed in the CdI_2 single crystals. Uncolored CdI_2 : CuI shows luminescence similar to CdI_2. Optically colored CdI_2 : CuI does not show luminescence, due to the presence of optically induced luminescence killing centers.

1. Introduction

In recent years the interest in nonsilver photographic materials has grown rapidly, due to the high expense and the shortage of silver. However, thus far no material has been found which produces the high contrast provided by the photographic silver halides within reasonable exposure times.

In the literature the existence of many nonsilver photographic materials like PbX_2, CdX_2, SnX_2 (X = Cl, Br, I), CuI, etc. has been reported (*1–6*). Like in the silver halides, illumination of these compounds using light with an energy at least equal to the energy difference between the valence band and the conduction band results in the photoneutralization of the ions in these compounds (photolysis). Contrary to the silver halides, where the photographic properties are mainly due to the motion of electrons and interstitial silver ions (*7, 8*), the photographic properties of PbX_2 and CdX_2 are mainly due to the motion of holes and halide ions.

Experimental investigations of the photographic properties of CdX_2 : CuX have also been reported (*6, 9–14*). The absorption of ultraviolet light in crystals of $CdCl_2$: CuCl and $CdBr_2$: CuBr creates neutral Cu atoms and Cu^{2+} ions (*9, 11–14*). Moreover, in the illuminated crystals two-dimensional aggregates of Cu are present. Trotter *et al.* (*6*) demonstrated the presence of Cu aggregates, with a radius of about 10 nm, in $CdCl_2$: CuCl glasses.

The photochromic properties of CdI_2 : CuI were reported in 1911 by Herrmann (*15*). Martin (*10*) has shown in an irradiated

---

* Dedicated to John B. Goodenough.

† Present address: Philips Research Laboratories, P.O. Box 80,000, 5600 JA Eindhoven, The Netherlands.

0022-4596/88 $3.00

mixture of CdI_2 and CuI in a binder that metal aggregates are also present. Moreover, such an irradiated mixture can be developed. The presence of metal aggregates in irradiated photosensitive compounds is also known from the silver halides (print-out effect).

Despite the effort, relatively little is known about the mechanism of the photolysis of the nonsilver halides. In this paper, we report an experimental study of the photolysis of crystalline $CdI_2:CuI$, making use of optical absorption and photoluminescence spectroscopy, electron spin resonance, and magnetic susceptibility measurements.

2. Experimental Methods

CdI_2 was prepared from the elements (Koch & Light, 6 *N* Cd; and Merck, doubly sublimed I_2) in a sealed ampoule in a temperature gradient from about 50 to 350°C. In order to be able to control the iodine vapor pressure, one side of the ampoule was kept at a temperature of only 50°C (cold point method). CuI was prepared in the same way (Koch & Light, 5 *N* Cu) except the temperature gradient was from 50 to 425°C.

CdI_2 crystals containing 1–5 mole% CuI were grown by the Bridgman method. Large crystals with a yellow color were obtained. Because pure CdI_2 is colorless, the yellow color is ascribed to the presence of Cu^+. The Cu^+ was distributed inhomogeneously in the crystals, as shown by the non-uniform yellow color.

The exciton absorption spectra of $CdI_2:CuI$ were recorded using a Perkin–Elmer EPS-3T spectrophotometer equipped with a Torso–Vacuo flow cryostat. The other absorption spectra were recorded using a Carl–Zeiss PMQII spectrophotometer, equipped with a laboratory-built flow cryostat.

The photoluminescence spectra were obtained using laboratory-built equipment. The light of a 1000-W Xe arc (Oriel 6269) was dispersed by means of a Jobin–Yvon H-20 UV monochromator. The emitted light was dispersed by means of a Jobin–Yvon H-20 VIS monochromator. The sample was mounted in an Oxford Instruments MB4 cryostat.

The $CdI_2:CuI$ crystals were colored, using unfocused light of a 50-W tungsten lamp which was placed at a distance of about 0.2 m. The light used was not monochromatic. The crystals were illuminated for 10 min on both sides. Using optical filters we showed that only radiation with an energy larger than 2.75 eV colored the $CdI_2:CuI$ crystals at temperatures above about 200 K.

3. Experimental Results

We have measured the absorption spectra of single-crystal platelets of $CdI_2:CuI$ for light propagating along the crystallographic *c* axis. The spectra show the absorption edges of CdI_2 near 3.5 eV, and in addition several broad absorption bands in the spectral region between 0.5 and 3.5 eV. The crystals with a higher CuI content also showed two sharp absorption peaks at 3.073 and 3.123 eV, with an intensity ratio of about 3 to 1 (Fig. 1).

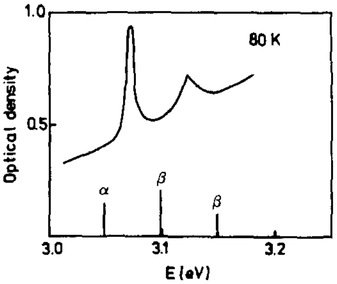

FIG. 1. Absorption spectrum of $CdI_2:CuI$ (3 mole% of CuI) at 80 K. The spectral resolution is 0.005 eV. The crystal had a thickness of 400 μm. The lines in the lower part give the position of exciton peaks in α-CuI and β-CuI.

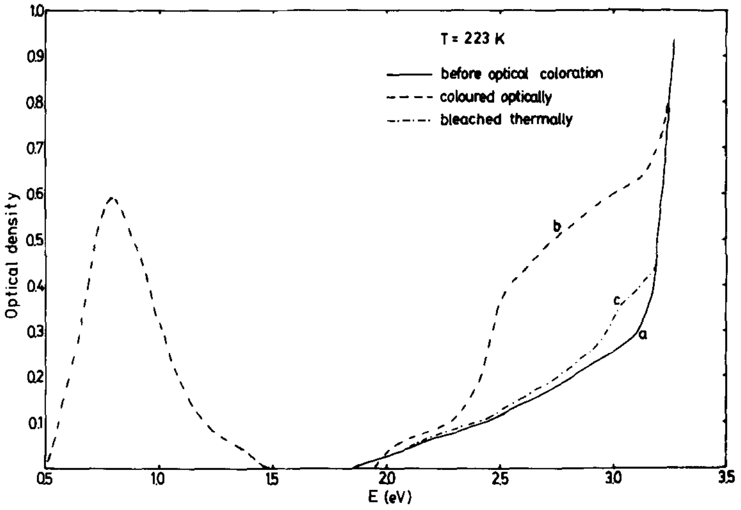

FIG. 2. Absorption spectrum of $CdI_2:CuI$ (1 mole% of CuI) at 223 K. The crystal had a thickness of 1250 μm.

The absorption spectrum at 223 K of a $CdI_2:CuI$ crystal with a thickness of 1250 μm containing 1 mole% CuI is shown in Fig. 2. Curve a is the spectrum of uncolored $CdI_2:CuI$. Note that the sharp peaks of Fig. 1 are not present in this spectrum. Above about 1.9 eV there is a broad optical absorption, whereas CdI_2 is transparent up to 3.5 eV. Curve b is the spectrum of optically colored $CdI_2:CuI$. Extra absorption appears in the energy region 0.5–1.5 eV (a band with an onset at 0.5 eV and a maximum at 0.8 eV) and continuous absorption in the region 1.9–3.2 eV. Curve c is the spectrum of $CdI_2:CuI$, bleached thermally by heating at 425 K for 10 min.

The spectra of $CdI_2:CuI$ change as a function of the number of times that the crystals are optically colored at 225 K and thermally bleached at 425 K for 10 min. After four of these cycles, a new absorption band with an onset at about 0.9 eV and a maximum at about 1.35 eV is observed in addition to the absorption band at 0.8 eV. The absorption band at 0.8 eV disappears at a much lower temperature than the new absorption band at 1.35 eV (Fig. 3).

We have investigated the kinetics of the various processes involved in the coloration by measuring the intensity of the extra absorption bands as a function of illumination time, and the decay in time of these bands. The results are presented and discussed in Section 6.

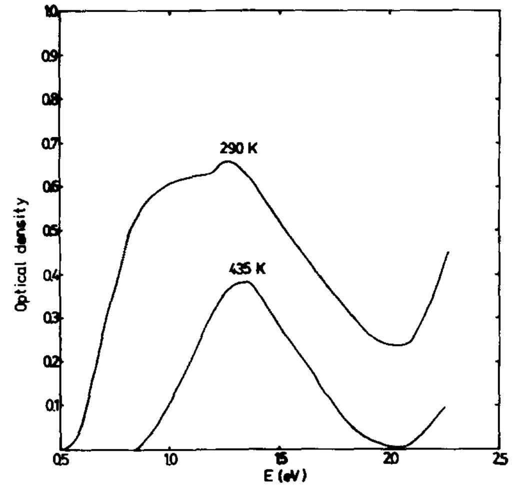

FIG. 3. Absorption spectrum of $CdI_2:CuI$ (1 mole% of CuI) at 290 and 435 K, after many optical coloration–thermal bleaching cycles.

Cu^{2+} ions are magnetic (spin $s = \frac{1}{2}$) and contribute to the magnetic susceptibility and electron spin resonance. In order to determine the possible presence of Cu^{2+} we measured the magnetic susceptibility of a crystal of $CdI_2:CuI$ (5 mole% CuI) before and after it had been colored optically. In the temperature region 4–125 K, the magnetic susceptibility was nearly independent of temperature and there was no significant difference between the two magnetic susceptibility measurements. Moreover, in electron spin resonance measurements on an optically colored $CdI_2:CuI$ single crystal (5 mole% CuI) at 100 and 300 K with a magnetic field of about 3000 G and a frequency of 9.1 GHz, no signal due to Cu^{2+} ions could be detected.

We have also optically colored $CdI_2:CuI$ (5 mole% CuI) in the presence of CCl_4. During and after optical coloration, the liquid CCl_4 was colored. This clearly proves that I_2 is formed during the optical coloration process: molecular iodine I_2 leaves the crystal and dissolves in CCl_4.

When a $CdI_2:CuI$ single crystal is colored optically using high-intensity radiation (we used the unfocused, nonmonochromatic light of a 300-W Varian VIX 300 Xe arc at a distance of about 0.1 m from the crystal) the crystal can no longer be thermally bleached because I_2 has evaporated from the crystal.

The luminescence spectra of a $CdI_2:CuI$ single crystal containing 5 mole% CuI are shown in Fig. 4. The emission spectra were recorded with a spectral resolution of about 0.02 eV. The luminescence was activated with light with an energy of 3.54 eV (spectral width 0.04 eV). The luminescence spectra of $CdI_2:CuI$ with 1 mole% CuI are very similar.

When $CdI_2:CuI$ is colored optically, no luminescence is observed, not even at low temperature ($T = 5$ K). After the crystal has been bleached, the luminescence can be observed again.

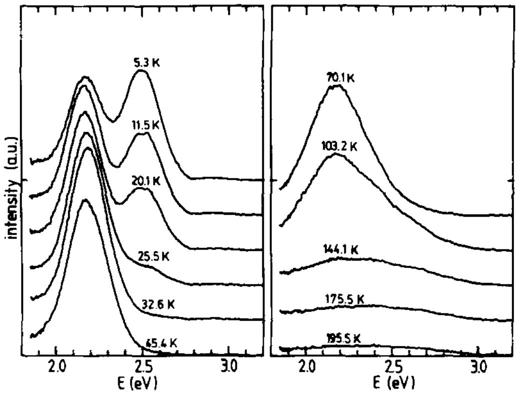

FIG. 4. Luminescence of uncolored $CdI_2:CuI$ (5 mole% of CuI).

4. Exciton Peaks of CuI in the Spectrum of $CdI_2:CuI$

The sharp peaks observed in the absorption spectrum of $CdI_2:CuI$ (Fig. 1) are absent in pure CdI_2. Moreover, these peaks are not observed in crystals which have been colored optically and bleached thermally.

Solid CuI crystallizes in several different modifications: β-CuI has the hexagonal wurtzite structure, α-CuI has the cubic zinc blende structure. In α-CuI two exciton peaks are observed at 3.05 and 3.75 eV (*21*). The excitons involved consist of an electron in the conduction band bound to a hole in the valence band. The valence band has mainly I 5*p* character. The top of the valence band is split into Γ_8 and Γ_7 states, due to spin–orbit coupling. The exciton at 3.75 eV involves a hole in the Γ_7 state, and the exciton at 3.05 eV a hole in the Γ_8 state.

Due to the hexagonal symmetry in β-CuI the Γ_8 valence band splits into two components transforming as Γ_4 and Γ_5 (in point group C_{3v}); the Γ_7 valence band transforms as Γ_4. The exciton involving the Γ_5 state is observed at 3.100 eV, the exciton involving the Γ_4 state (derived from Γ_8) at 3.148 eV (*21*). From the basis functions for the Γ_4 and Γ_5 valence band states one easily deduces

TABLE I

SPLITTING OF THE I 5*p* VALENCE BAND IN α-CuI DUE TO SPIN–ORBIT COUPLING (POINT GROUP T_d), AND IN β-CuI DUE TO SPIN–ORBIT COUPLING AND A TRIGONAL CRYSTAL FIELD (POINT GROUP C_{3v})

T_d	C_{3v}	I(E⊥c)	I(E//c)
Γ_8 (j = 3/2)	Γ_5 (m_j = ±3/2)	1	0
	Γ_4 (m_j = ±1/2)	1/3	2/3
Γ_7 (j = 1/2)	Γ_4 (m_j = ±1/2)	2/3	1/3

Note. The + and − in the basis functions refer to the electron spin direction.

the intensity ratio of excitons Γ_4 and Γ_5 for light propagating along the *c* axis. The results are given in Table I. We have neglected mixing between the two Γ_4 states; however, only little mixing is expected because the trigonal crystal field is small compared to the spin–orbit splitting.

The observed intensity ratio of the peaks in $CdI_2:CuI$ at 3.123 and 3.073 eV, for light propagating along the *c* axis, is 0.3. The observed splitting of 0.050 eV is almost equal to the splitting of 0.048 eV of the exciton peaks in β-CuI. Moreover, the shapes of the exciton peaks are very similar. These observations strongly indicate that the observed sharp peaks in the spectrum of $CdI_2:CuI$ are the exciton peaks of β-CuI present in the sample. The stable modification of CuI below 643 K is α-CuI. Apparently, the metastable hexagonal phase β-CuI is more easily formed by internal precipitation in the hexagonal CdI_2 lattice.

Due to the small size of the β-CuI microcrystals, the excitons of CuI in CdI_2 may have an energy slightly different from the excitons in pure CuI (*22*). The energy difference may also be caused by strain effects (*23*).

The observation of the exciton peaks of β-CuI indicates that CuI is not completely soluble in CdI_2. Herrmann (*15*) reported a study of the phase diagram of $CdI_2:CuI$. He observed that CdI_2 and CuI were completely miscible at the temperatures where the crystals were grown. Our results indicate that at lower temperatures β-CuI precipitates in the CdI_2 lattice. Another investigation of the phase diagram of $CdI_2:CuI$ would be worthwhile.

After the optical coloration–thermal bleaching process, the excitons of CuI have disappeared. This indicates that at least a large part of the Cu ions is dissolved in the CdI_2 lattice.

5. The Mechanism of Optical Coloration

The photochromic properties of $CdCl_2:CuCl$ and $CdBr_2:CuBr$ are due to the transfer of electrons from one Cu^+ to another Cu^+, leading to the formation of neutral Cu atoms and Cu^{2+} ions (*9, 11–14*). The presence of Cu^{2+} ions was demonstrated with electron spin resonance. We will show that the mechanism of the photochromic process in $CdI_2:CuI$ is different, and does not involve Cu^{2+} ions.

The values of the crystal field splitting 10 Dq of CoI_2 (0.806 eV) and NiI_2 (0.950 eV) (*24*) indicate that the crystal field *d–d* transition $^2E_g \rightarrow {}^2T_{2g}$ of Cu^{2+} surrounded octahedrally by iodine ions is expected at about 1 eV. This means that the absorption bands at 0.8 and 1.35 eV could possibly be due to the *d–d* transition $^2E_g \rightarrow {}^2T_{2g}$ of Cu^{2+} surrounded octahedrally by iodine ions at two different types of sites. However, electric dipole *d–d* transitions are parity forbidden in octahedral symmetry, resulting in a very low transition probability. A crude calculation shows that almost all Cu^+ ions need to be converted into Cu^{2+} ions in the optical coloration process if the observed absorption is due to Cu^{2+}. This is in contradiction to the magnetic susceptibility and the electron spin resonance measurements.

When Cu^{2+} ions are surrounded tetrahedrally by iodine ions, the *d–d* transitions are parity allowed. However, in this case

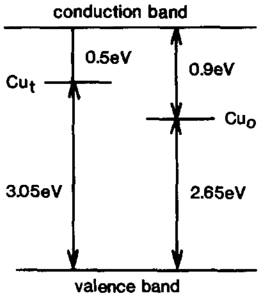

FIG. 5. Energy level diagram of Cu atoms in tetrahedral (Cu_t) and octahedral (Cu_O) sites in CdI_2.

the *d–d* crystal field transition $^2T_{2g} \rightarrow {}^2E_g$ of Cu^{2+} is expected at a much lower energy because of the smaller crystal field splitting 10 Dq in tetrahedra.

We ascribe the extra absorption bands at 0.8 and 1.35 eV to the presence of two different types of neutral Cu atoms. The extra absorption bands are due to the transition of electrons from neutral Cu atoms to the conduction band of CdI_2. The optical coloration can be written as a chemical reaction:

$$Cu^+ + I^- \xrightarrow{h\nu} Cu^0 + I^0. \qquad (1)$$

We suggest that the absorption band at 0.8 eV is due to Cu atoms which are tetrahedrally surrounded by I^- ions, and the absorption band at 1.35 eV to Cu atoms which are octahedrally surrounded by I^- ions (Fig. 5). Notice that the thermal ionization energy which corresponds to the distance of the energy level from the conduction band edge corresponds to the onset of the absorption band for optical ionization.

Optical coloration of $CdI_2:CuI$ single crystals occurs only for radiation with an energy greater than 2.75 eV. This value agrees quite well with the energy needed to excite an electron from the valence band into the Cu_O level.

In the following we will show that the optical absorption in an optically colored $CdI_2:CuI$ crystal (Fig. 2) in the region 1.9–3.2 eV is due to the presence of Cu aggregates. We will use a modification of the theory of Mie (*6, 25*).

When the mean radius of the Cu aggregates is much smaller than the wavelength of the incident light, the effective dielectric constant ε_{eff} of a composite containing ellipsoidal Cu aggregates is given by

$$\varepsilon_{eff} = \varepsilon_{\infty\perp}\left\{1 + \frac{3F(\varepsilon_\perp - \varepsilon_{\infty\perp})}{L_\perp\varepsilon + (1 - L_\perp)\varepsilon_{\infty\perp}}\right\}, \qquad (2)$$

where F is the volume fraction occupied by the Cu aggregates and $L_\perp$ is the depolarization factor for fields perpendicular to the singular axis of the ellipsoid. The depolarization factors for ellipsoids have been calculated by Osborn (*26*). $\varepsilon_{\infty\perp}$ is the dielectric constant of CdI_2 for electric fields perpendicular to the *c* axis and $\varepsilon_\perp$ is the dielectric constant of the Cu aggregates perpendicular to the singular axis of the ellipsoid at the frequency of the light. We assume that the singular axis of the Cu ellipsoids is parallel to the crystallographic *c* axis of the matrix CdI_2.

If the size of the Cu particles is comparable to the mean free path of the conduction electrons, the optical response of these electrons is modified by boundary scattering. This leads to a change of the dielectric constant of Cu.

The dielectric constant of Cu has interband (ε^i) and conduction electron (ε^D) contributions:

$$\varepsilon = \varepsilon^i + \varepsilon^D. \qquad (3)$$

ε^D is given by Drude theory

$$\varepsilon^D = 1 - \frac{\omega_p^2\tau^2}{1 + \omega^2\tau^2} + i\,\frac{\omega_p^2\tau}{\omega(1 + \omega^2\tau^2)}, \qquad (4)$$

where ω_p is the plasma frequency, τ is the relaxation time for conduction electron scattering, and $\omega = 2\pi c/\lambda$. The relaxation time for boundary scattering τ_s in a given direction depends on the particle size in that direction (*6*):

$$\tau_s = D/v_F, \tag{5}$$

where D is the dimension of the particle in that direction and v_F is the Fermi velocity. The total relaxation time for conduction electron scattering is given by

$$\frac{1}{\tau} = \frac{1}{\tau_B} + \frac{1}{\tau_s} \tag{6}$$

where τ_B is the relaxation time for conduction electron scattering in bulk Cu (without boundary scattering).

The dielectric constant of a Cu particle can be written as

$$\varepsilon = \varepsilon_B + (\varepsilon^D - \varepsilon_B^D), \tag{7}$$

where ε_B is the dielectric constant of bulk Cu (without boundary scattering). The conduction electron contributions ε^D and ε_B^D are obtained from Eq. (4) by substituting relaxation times τ and τ_B, respectively. The absorption coefficient α is given by $\alpha = 2\pi\varepsilon_2/n\lambda$, where ε_2 and ε_1 are the imaginary and real parts of the complex dielectric constant, respectively, $n = \sqrt{\varepsilon_1}$ is the refractive index and λ is the wavelength of the light.

In the calculations we used values $\omega_p = 1.34 \times 10^{16}$ sec^{-1} and $\tau_B = 6.87 \times 10^{-15}$ sec (298 K) for bulk copper (*25*). The Fermi velocity of Cu is $v_F = 1.57 \times 10^6$ m sec^{-1} (*27*). The dielectric constant ε_B of bulk copper as a function of frequency was calculated using data from Ref. (*28*).

In the calculations we assumed that the Cu aggregates are flat disks; i.e., we assumed an ellipsoidal shape with the axis parallel to the c axis much shorter than the axis in the ab plane. These assumptions are consistent with the layer structure of CdI_2. The Cu aggregates in $CdCl_2:CuCl$ and $CdBr_2:CuBr$ also have the proposed nearly two-dimensional character (*11, 14*).

Because the direction of the incident light was parallel to the crystallographic c axis, there is only electric polarization in the ab plane. The depolarization factor L in that direction for an ellipsoid with a and b radii equal and larger than the c radius is given by (*26*)

$$L = \frac{1}{2(m^2 - 1)} \left[m^2(m^2 - 1)^{-1/2} \times \arcsin \left\{ \frac{(m^2 - 1)^{1/2}}{m} \right\} - 1 \right], \tag{8}$$

where $m = a/c$. For flat disks $m \gg 1$ and $L = 0$. The high-frequency dielectric constant of CdI_2 for light polarized perpendicular to the c axis is $\varepsilon_{\infty\perp} = 4.6$ (*29*).

We have performed a series of calculations, in which the c radius of the ellipsoid was fixed and the $a = b$ radius was varied. A change of the volume fraction F did not alter the shape of the curve of the absorption coefficient α as a function of the energy. The results of the calculations are plotted in Fig. 6. The measured absorption coefficient is given in Fig. 7. The calculations show that reasonable agreement between the observed and calculated absorption coefficients as a function of energy is obtained only for highly anisotropic Cu aggregates. Unfortunately the calculated absorption coefficient as a function of energy is rather insensitive to the size of the ellipsoid. We believe, on the basis of the layer structure of CdI_2, that it is not very likely that the Cu aggregates are thicker than a small number of monolayers of Cu atoms. Therefore, the estimated mean size of the Cu aggregates is of the order of $100 \times 100 \times 8$ Å^3. The volume fraction of the Cu aggregates needed to obtain quantitative agreement between the calculated and the observed absorption coefficients is of the order of 10^{-6}. This corresponds to a small fraction of Cu atoms (about 0.3%) involved in the aggregation process.

Note that for metal particles of finite size the electron energy levels no longer form continuous energy bands, but rather form

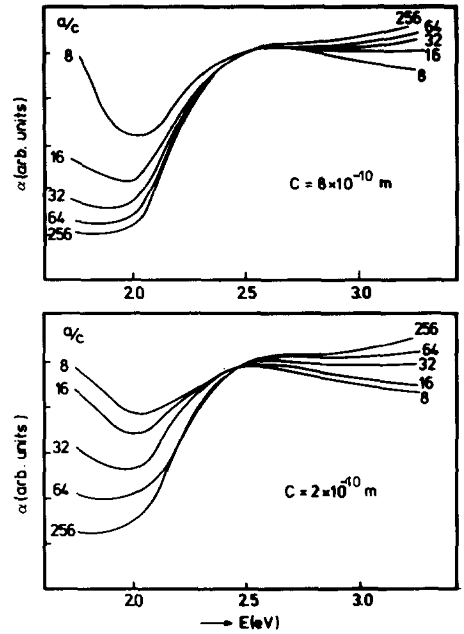

FIG. 6. Calculated absorption coefficients α of CdI_2 containing ellipsoidal Cu particles. In each plot the c axis of the ellipsoid is constant. The numbers for the different curves give the ratio $m = a/c$. The curves are scaled to one another with the volume fraction F.

discrete energy levels. For very small particles the energy difference between the energy levels becomes significant (*6, 30*). Kreibig has pointed out that for silver particles this effect can be neglected unless the particles consist of less than 400 atoms (*31*). Smithard found that this effect can be neglected even for a substantially smaller number of Ag atoms in the particles (*32*). We expect these results to apply also to the Cu aggregates. The mean number of Cu atoms in the Cu aggregates is about 10^4, indicating that the assumptions used are valid.

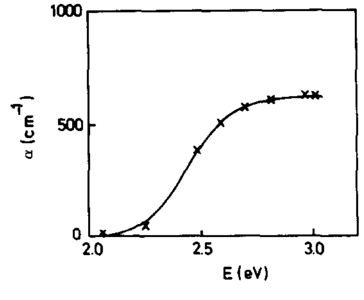

FIG. 7. Absorption coefficient α of Cu aggregates in CdI_2.

6. Kinetics of Coloration and Thermal Bleaching

We determined the rate of the optical coloration process by measuring the intensity of the extra absorption band at 0.8 eV as a function of illumination time. We found that the rate of coloration increases slowly with increasing temperature. The data are not very accurate. The increase corresponds to an activation energy of about 0.2 eV. Almost the same value, $E_a = 0.18$ eV, is reported for the activation energy of the photolysis of CdI_2 (*33*). The rate-determining step in the photolysis of PbI_2 and SnI_2 is thermally activated anion vacancy diffusion (*2, 3*). This could also be the rate-determining step in the coloration process of CdI_2 : CuI. The coloration process would then proceed in the following way. Optical excitation of CdI_2 produces photoelectrons and photoholes. The photoelectrons in CdI_2 : CuI are captured by Cu^+ ions and the photoholes by I^- ions. The recombination of these charges is prevented at higher temperatures by thermally activated hole diffusion. The holes diffuse to the surface, I_2 molecules evaporate from the crystal, and anion vacancies diffuse into the crystal. Thus the trapping of the photoelectrons by the Cu^+ ions is the precursor of the photolysis.

We also measured the intensity of the absorption bands at 0.8 and 1.35 eV as a function of time at different temperatures. The intensity I of these peaks shows an exponential decay $I = I_0 \exp(-t/\tau)$. The relaxation time τ depends on temperature according to an Arrhenius law $\tau = \tau_0$

TABLE II

INTENSITY (I) OF THE ABSORPTION BAND AT 0.8 eV FOR A CRYSTAL WITH THICKNESS $d = 900\ \mu m$ AS A FUNCTION OF ANNEALING TIME t (RELAXATION TIME τ IS DEFINED BY AN EXPONENTIAL DECAY $\exp(-t/\tau)$)

(a) $T = 382$ K			$1/\tau = 2.4 \times 10^{-4}\ sec^{-1}$		
t_s	0	240	540	1020	
I	1	0.93	0.85	0.78	
(b) $T = 398$ K			$1/\tau = 5.0 \times 10^{-4}\ sec^{-1}$		
t_s	0	240	480	740	960
I	1	0.90	0.79	0.69	0.63
(c) $T = 421$ K			$1/\tau = 9.7 \times 10^{-4}\ sec^{-1}$		
t_s	0	180	420	660	900
I	1	0.82	0.65	0.53	0.41

$\exp(E_0/kT)$, with ativation energy E_0. The observed data are given in Tables II and III and Fig. 8. We obtained an activation energy of 0.49 ± 0.03 eV for thermal bleaching of the band at 0.8 eV, and an activation energy of 1.01 ± 0.06 eV for thermal bleaching of the band at 1.35 eV.

We ascribe the thermal bleaching process to the conversion of neutral Cu atoms and I_2 molecules or I_2^- self-trapped holes to Cu^+ and I^- ions. The rate-determining step is the thermal ionization of the neutral Cu localized centers. The activation energy for the thermal bleaching is smaller than the energy where the corresponding absorption bands have their maxima. This is due to the fact that in the absorption process there is no lattice relaxation whereas in the thermal bleaching process lattice relaxation may occur (Franck–Condon principle). Indeed the thermal activation energies of 0.49 and 1.01 eV are close to the corresponding onsets, which are 0.5 and 0.9 eV, respectively (see Fig. 3).

The behavior of the absorption band due to the presence of Cu aggregates is in qualitative agreement with this model. The aggregation of neutral Cu atoms only takes place if the total energy of the aggregate is smaller than the sum of the energies of isolated Cu atoms. Therefore one expects a higher activation energy for the dis-

TABLE III

INTENSITY I OF THE ABSORPTION BAND AT 1.35 eV FOR A CRYSTAL WITH THICKNESS $d = 1250\ \mu m$ AS A FUNCTION OF ANNEALING TIME t (RELAXATION TIME τ IS DEFINED BY AN EXPONENTIAL DECAY $\exp(-t/\tau)$)

(a) $T = 399$ K			$1/\tau = 1.9 \times 10^{-4}\ sec^{-1}$				
t_s	0	600	1200	2400	3600	6600	8400
I	1	0.87	0.76	0.59	0.46	0.26	0.20
(b) $T = 423$ K			$1/\tau = 9.6 \times 10^{-4}\ sec^{-1}$				
t_s	0	300	600	900	1200	1800	
I	1	0.72	0.53	0.38	0.28	0.16	
(c) $T = 428$ K			$1/\tau = 1.1 \times 10^{-3}\ sec^{-1}$				
t_s	0	300	540	780			
I	1	0.80	0.55	0.45			
(d) $T = 443$ K			$1/\tau = 3.7 \times 10^{-3}\ sec^{-1}$				
t_s	0	240	470				
I	1	0.27	0.18				

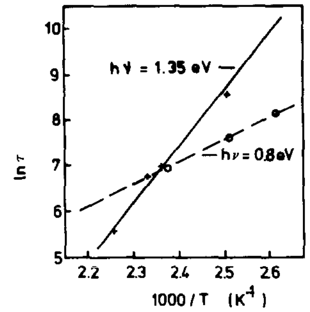

FIG. 8. Plot of ln τ versus reciprocal temperature for thermal bleaching of the absorption bands at 0.8 and 1.35 eV. The activation energies are 0.49 ± 0.03 and 1.01 ± 0.06 eV, respectively.

appearance of the absorption bands due to these aggregates than for the disappearance of the absorption band due to the presence of the isolated Cu atoms. This is observed indeed. In Fig. 2 the absorption band due to the presence of the Cu aggregates has not completely disappeared, whereas the absorption band at 0.8 eV due to the presence of isolated Cu atoms has disappeared competely. The same behavior was observed with respect to the other absorption band at 1.35 eV.

7. Luminescence of $CdI_2:CuI$

The luminescence peaks observed in $CdI_2:CuI$ are also found in pure CdI_2 (*16–20*), but with different relative intensities. No new emission peaks, typical for the presence of copper, were observed. Thus the luminescent processes in $CdI_2:CuI$ are the same as in pure CdI_2, but the kinetics and quenching of the luminescence are influenced by copper.

As in CdI_2 the two broad emission bands at 2.16 and 2.50 eV are ascribed to self-trapped excitons involving holes in I 5*p* orbitals and electrons in Cd 5*s* orbitals (*20*).

A striking difference between the luminescence spectra of $CdI_2:CuI$ and CdI_2 at low temperature ($T < 40$ K) is the absence of sharp exciton emissions in $CdI_2:CuI$. This is in agreement with results obtained by Lyskovich *et al.* (*36*). These authors observed a strong quenching of the ultraviolet emission of CdI_2 due to impurities at 3.37 eV. Therefore we ascribe the quenching of the ultraviolet luminescence to the presence of Cu ions in $CdI_2:CuI$. The excitation energy probably is transferred to Cu^+, followed by nonradiative decay on Cu^+.

A second difference between the luminescence of $CdI_2:CuI$ and CdI_2 is the different relative intensity of the broad emission at 2.16 and 2.50 eV at low temperature ($T < 40$ K), and the smaller intensity in the spectral region between the two bands. This is probably due to a smaller inhomogeneous broadening of the emission bands in $CdI_2:CuI$.

The thermal quenching of the emission band at 2.50 eV is more rapid in $CdI_2:CuI$ than in pure CdI_2. This must be due to an enhanced transfer of energy from the self-trapped excitons to states of Cu^+ and subsequent decay (the Cu^+ ion itself shows no visible luminescence).

Above 35 K the intensity of the emission band at 2.16 eV decreases with increasing temperature. The shift of the emission to higher energy observed in pure CdI_2 with increasing temperature above 70 K is observed to a far lesser extent in the emission spectra of $CdI_2:CuI$. The absence of intense luminescence in the blue part of the spectrum in the temperature region 70–200 K and the thermal quenching of the emission band at 2.16 eV above 35 K must be due, again, to energy transfer to the Cu ions.

At temperatures above about 200 K, the luminescence of $CdI_2:CuI$ is quenched completely, just as in pure CdI_2 (*20*). This quenching of the luminescence of CdI_2 is ascribed to the partial photolysis of the compound, resulting in the production of luminescence killing I atoms or I_2^- molecular ions. The same mechanism will also be present in $CdI_2:CuI$. However, the photolysis process in $CdI_2:CuI$ also produces neutral Cu atoms, which may also be involved in the quenching process. Indeed, the temperature quenching of the luminescence above 50 K is more rapid in $CdI_2:CuI$ than in pure CdI_2, indicating that in $CdI_2:CuI$ the I atoms or the I_2^- molecular ions are not the only luminescence-killing centers.

The complete absence of luminescence in optically colored $CdI_2:CuI$, even at low temperature ($T = 5$ K), must be due to the photolysis that has taken place in optically colored $CdI_2:CuI$. The photolysis results in neutral Cu atoms and I atoms or I_2^- molecular ions. The photolysis yield in $CdI_2:CuI$ is much larger than in CdI_2. The quenching of the luminescence of optically colored $CdI_2:CuI$ is due to the presence of Cu atoms or to the presence of I atoms or I_2^- molecular ions. The photoelectrons and the photoholes recombine either on the Cu atoms or on the I atoms or I_2^- molecular ions.

We remark that, contrary to uncolored $CdI_2:CuI$ crystals, optically colored $CdI_2:CuI$ crystals do not show photoconductivity (*37*). This again indicates the presence of efficient centers for electron–hole recombination.

8. Conclusions

We have shown that $CdI_2:CuI$ is photochromic. When the compound is illuminated with blue or ultraviolet light, extra absorption bands appear in the near-infrared and visible parts of the spectrum. The absorption bands in the near-infrared are due to the presence of neutral Cu atoms at octahedral and tetrahedral sites, whereas the band in the visible is due to Cu aggregates. In as-grown crystals of $CdI_2:CuI$ (3 mole% CuI) sharp exciton peaks are observed as a consequence of the presence of microcrystals of β-CuI. After one optical coloration–thermal bleaching cycle these exciton peaks are no longer observed because the Cu^+ ions have dissolved in the CdI_2 lattice.

The optical coloration of $CdI_2:CuI$ is ascribed to the optical transfer of electrons from I^- to Cu^+, leading to neutral Cu atoms and I atoms. The separation of these charges is the rate-determining step of the coloration process, and proceeds by hole diffusion. The thermal bleaching is due to the thermal excitation of electrons from the Cu atoms to the conduction band.

The mechanism of photochromism in $CdI_2:CuI$ is different from that in $CdCl_2:CuCl$ and $CdBr_2:CuBr$. In the chloride and bromide systems Cu^{2+} ions are formed optically; this is not the case in $CdI_2:CuI$. the reason is that Cu^{2+} ions are not stable in an iodide matrix; any Cu^{2+} present would reduce I^- ions as $Cu^{2+} + I^- \rightarrow Cu^+ + I^0$. This is also the reason that $CuCl_2$ and $CuBr_2$ are stable compounds, and the reason that CuI_2 does not exist (*38*).

The luminescence spectrum of uncolored (or thermally bleached) $CdI_2:CuI$ single crystals consists of two broad emission bands which are also observed in the luminescence spectrum of CdI_2. Optically colored $CdI_2:CuI$ does not show luminescence, due to the presence of optically generated luminescence-killing centers.

References

1. J. Malinowski, *Photogr. Sci. Eng.* **15,** 175 (1971).
2. M. G. Albrecht and M. Green, *J. Phys. Chem. Solids* **38,** 297 (1977).
3. M. Green and T. A. Kuku, *J. Phys. Chem. Solids* **44,** 999 (1983).
4. R. A. Fotland, *Chem. Phys. Lett.* **33,** 957 (1960).
5. M. T. Kostyshir, E. V. Mihailovskaya, and P. F. Romanenko, *Sov. Phys. Solid State* **8,** 451 (1966).
6. D. M. Trotter, J. W. H. Schreurs, and P. A. Tick, *J. Appl. Phys.* **53,** 4657 (1982).

7. N. F. Mott and R. W. Gurney, "Electronic Processes in Ionic Crystals," Oxford Univ. Press (Clarendon), London/New York (1940).
8. F. C. Brown, "Treatise on Solid State Chemistry" (N. B. Hannay, Ed.), Vol. IV, p. 333, Plenum Press, New York (1976).
9. K. Kan'no, S. Naoe, S. Mukai, and Y. Nakai, *Solid State Commun.* **13,** 1325 (1973).
10. T. W. Martin, U.S. Patent No. 3,996,053 (1976).
11. S. Naoe, K. Kan'no, and Y. Nakai, *J. Phys. Soc. Japan* **42,** 1609 (1977).
12. S. A. Payne and D. S. McClure, *J. Phys. Chem.* **88,** 1379 (1984).
13. S. A. Payne and D. S. McClure, "Photochem. and Photobiol." (A. Zewail, Ed.), Vol. II, p. 1129, Harwood Acad. Pub., New York (1983).
14. H. Matsumoto, H. Nakagawa, and H. Kuwabara, *J. Phys. Soc. Japan* **44,** 957 (1978).
15. G. Herrmann, *Z. Anorg. Chem.* **71,** 257 (1911).
16. H. Matsumoto and H. Nakagawa, *J. Luminescence* **18/19,** 19 (1979).
17. H. Nakagawa, H. Murata, and H. Matsumoto, *J. Luminescence* **24/25,** 652 (1981).
18. H. Nakagawa and H. Matsumoto, *Physica B* **105,** 83 (1981).
19. H. Matsumoto, H. Nakagawa, and S. Kondo, *Memo. Fac. Engin. Fukui Univ.* **31,** 53 (1983).
20. C. R. Ronda, J. H. van der Meer, A. A. van Heuzen, and C. Haas, *J. Solid State Chem.*, in press.
21. M. Cardona, *Phys. Rev.* **129,** 69 (1963).
22. T. Tsuboi, *J. Chem. Phys.* **72,** 5343 (1980).
23. A. Blacha, N. E. Christensen, and M. Cardona, *Phys. Rev. B* **33,** 2413 (1986).
24. S. R. Kuindersma, thesis, University of Groningen (1980).
25. S. Garoff and C-D. Hanson, *Appl. Optics* **20,** 758 (1981).
26. F. A. Osborn, *Phys. Rev.* **67,** 351 (1945).
27. C. Kittel, "Introduction to Solid State Physics" 5th ed., Wiley, New York (1976).
28. P. B. Johnson and R. W. Christy, *Phys. Rev. B* **6,** 4370 (1972).
29. H. J. L. van der Valk, thesis, University of Groningen (1978).
30. A. Kawabata and R. Kubo, *J. Phys. Soc. Japan* **21,** 1765 (1966).
31. U. Kreibig, *J. Phys. F* **4,** 999 (1974).
32. M. A. Smithard, *Solid State Commun.* **13,** 153 (1973).
33. A. B. Lyskovich, V. D. Bondar, and Yu. V. Karavan, *Ukr. Fiz. Zh.* **24,** 401 (1979).
34. Ch. B. Lushchik, I. K. Vitol, and M. A. Elango, *Sov. Phys. Usp.* **20,** 489 (1977).
35. Y. Toyozawa, *Appl. Optics* **19,** 4101 (1980).
36. A. B. Lyskovich and M. R. Panasyuk, *Ukr. Fiz. Zh.* **28,** 135 (1983).
37. C. R. Ronda, E. Zwaal, and C. Haas, unpublished results.
38. G. van der Laan, C. Westra, C. Haas, and G. A. Sawatzky, *Phys. Rev. B* **23,** 4389 (1981).